Revista de Metalurgia
April-June 2021, 57 (2), e196
ISSN-L: 0034-8570
https://doi.org/10.3989/revmetalm.196

Improvement of mechanical properties of aluminum base composite reinforced by steel Ck75 wire through explosive welding

Maryam Roudbari[a], Nima Refahati[b,*], Ali Mehdipour[a]

[a] Renewable Energy Research Center, Damavand Branch, Islamic Azad University, Damavand, Iran

[b] Department of Mechanical Engineering, Damavand Branch, Islamic Azad University, Damavand, Iran

(*Corresponding author: refahati@damavandiau.ac.ir)

Submitted: 18 December 2020; Accepted: 4 March 2021; Available On-line: 28 June 2021

ABSTRACT: The explosive welding is applicable in a wide variety of thicknesses, thermal, and mechanical properties, which has different applications. In this paper, Aluminum base composite as reinforcement with Steel Ck75 wire was manufactured by explosive welding. The Steel Ck75 wires were placed between two Aluminum plates. The Steel Ck75 wire was used to increase the strength of the Aluminum base composite. The parameters of the process were evaluated in detail. The excellent bonding quality of the interface without void can be represented in light microscope images. The weldability window and the simulation with the experimental data confirmed the fact that material and process parameters were well selected. The tensile tests showed that the reinforced composite showed higher strength than the unreinforced composite of about 8%.

KEYWORDS: Al 1050; Steel CK75; Simulation; Weldability Window

Citation/Citar como: Roudbari, M.; Refahati, N.; Mehdipour, A. (2021). "Improvement of mechanical properties of aluminum base composite reinforced by steel Ck75 wire through explosive welding". *Rev. Metal.* 57(2): e196. https://doi.org/10.3989/revmetalm.196

RESUMEN: *Mejora de las propiedades mecánicas del compuesto base de aluminio reforzado con alambre de acero Ck75 mediante soldadura explosiva.* La soldadura explosiva es aplicable en una amplia variedad de espesores, propiedades térmicas y mecánicas, por lo que tiene diferentes aplicaciones. En este trabajo, el compuesto de base de aluminio como refuerzo con alambre de acero Ck75 fue fabricado mediante soldadura explosiva. Los alambres de acero Ck75 se colocaron entre dos placas de aluminio. El alambre Steel Ck75 se utilizó para aumentar la resistencia del compuesto de base de aluminio. Los parámetros del proceso se evaluaron en detalle. La excelente calidad de unión de la interfaz sin vacíos se puede representar en imágenes de microscopio óptico. El intervalo de soldabilidad y la simulación con los datos experimentales confirmaron que los parámetros del material y del proceso estaban bien seleccionados. Los ensayos de tracción mostraron que el material compuesto reforzado mostró una resistencia mayor que el material compuesto no reforzado de aproximadamente un 8%.

PALABRAS CLAVE: Acero CK75; Al 1050; Simulación; Intervalo de soldabilidad

ORCID ID: Maryam Roudbari (https://orcid.org/0000-0002-0433-8485); Nima Refahati (https://orcid.org/0000-0001-8965-3291); Ali Mehdipour (https://orcid.org/0000-0001-7382-3612)

1. INTRODUCTION

Improving the mechanical properties of materials with using micro and nano fiber are widespread. Polymer based composites are normally reinforced with nano fiber like carbon nano tube and boron nitride and show increasing in mechanical properties (Zarabimanesh *et al.,* 2021). The metal composites are completely different and continuous fiber play bold role. Aluminum base composites are lightweight engineering metals (Wagner, 2018). This composite is widely applied in aerospace, equipment manufacturing, chemical industries, etc. (Pakzaman and Divandari, 2012; Mavhungu *et al.*, 2017). It was fabricated in different methods by lost foam casting, hot rolling, and explosive welding (EXW) (Roudbari *et al.*, 2013; Sharma *et al.*, 2010; Guler *et al.*, 2014; Etemadi *et al.*, 2020).

The EXW is a type of welding process which can connect a base plate with a flyer plate by great pressure, that is manufactured by the detonation (Roudbari *et al.*, 2013). Aluminum base composites are reinforcement with SiC, carbon, Al_2O_3 fibers, and also Steel wire (Bhalla and Willams, 1977; Gülenc *et al.*, 2016; Huagui *et al.*, 2017).

The EXW is a solid-state process, that applied a controlled explosive detonation to enforce two or three metals together at great pressure (Bhalla and Willams, 1977). A system of the EXW process is shown in Fig. 1.

The EXW has that ability to bond different metals and has been used to manufactured some composite (Patterson, 1993; Roudbari *et al.*, 2013).

In the EXW, different phenomena such as plastic deformation of metals, great collision velocity, high temperature, and great-pressure states happen for a short time (Khanzadeh Gharah *et al.,* 2017). Thus, it seems that the finite element method helpful for measuring (Khanzadeh Gharah *et al.*, 2018; Deemyad *et al.*, 2020).

Zerui *et al.* (2020) studied the numerical simulation of Steel 1006- SS 304 was fabricated by the EXW. Roudbari *et al.* (2020) predicted parameters of the weldability window and the numerical simulation of Al base composite with reinforced Steel 1006. The experimental test was applied to verify the parameters of the simulation and the weldability window.

In the paper, pure Aluminum 1050 and Steel Ck75 chosen due to easier availability and their combination would permit the production of composite with good strength to weight ratio. The aim of this paper to manufacture Steel Ck75 wire reinforced Al base composite with improved mechanical properties. At present, the test of explosive welding was applied to validate the weldability window and simulation results.

2. MATERIALS AND METHODS

2.1. Explosive welding model

The simulation of the EXW process was used by AUTODYN version 18. In the current model, Steel Ck75 wires for reinforcing and Al1050 was selected as the flyer plate and the base. A model for Al1050/SteelCK75/Al1050 explosive welding simulation is displayed in (Fig. 2). The parallel system of the simulation is shown in (Fig. 2). The detonator is mounted on the surface edge of the Anfo.

The default units are applied in the simulation, i. e., the mass in mg, the length is mm, the time is ms. The model is comprised of four materials, i. e., Al1050, Steel Ck75, Al1050 and Anfo (ammonium-nitrate/fuel-oil). The geometry sized are shown in Table 1.

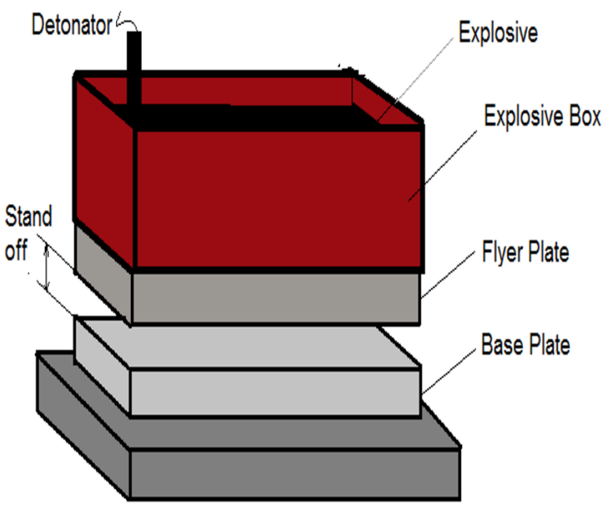

Figure 1. The EXW system.

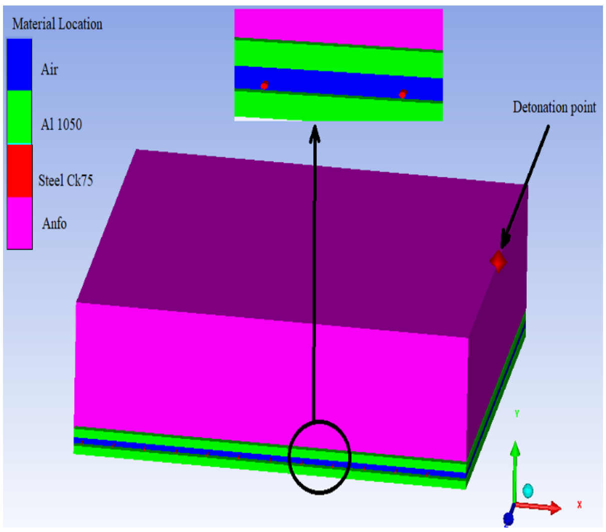

Figure 2. Simulation model of Al/Steel Ck75/Al.

Table 1. Geometry parameters of Al 1050, Steel Ck75, and Anfo in the simulation

Materials	Geometry (mm)
Anfo (Explosive)	250×250×60
Al 1050 (Flyer Plate)	250×250×4
Al 1050 (Base plate)	250×250×4
Steel Ck75	D=0.9

The flyer plate, the base plate, and reinforced were modeled by Johnson-Cook (JC) equation (Zerui *et al.,* 2020). It constitutive equation (Nassiri *et al.,* 2015) gives the Von-Misses yield stress as:

$$T_H = \frac{T - T_{room}}{T_{melt} - T_{room}} \quad (1)$$

$$Y = [A+B\varepsilon^n](1+C1n\varepsilon^*)[1-(T_H)^m] \quad (2)$$

where ε^*_p is the plastic strain-rate (often equal 1), ε is the equivalent plastic strain, is the homologous temperature, T is the absolute temperature. The five constants are A, B, C, m, n. The JC parameter and the mechanical properties of Al and Steel are described in Table 2. The material constants of JC were obtained from limited straining tests carried out in tension or torsion (Akbari Mousavi and Al-Hassani, 2008). The Jones-Wilkins-Lee (JWL) equation for the ANFO can be estimated as follows (Los *et al.*, 2010):

$$P = A\left(1-\frac{\omega}{R_1V}\right)\exp(-R_1V) + B\left(1-\frac{\omega}{R_2V}\right)\exp(-R_2V) + \frac{\omega E}{V} \quad (3)$$

where, P is the pressure, ע is the specific volume, E is internal energy. The five constants are C_1, C_2, r_1, r_2, ω as displayed in Table 3 (Zerui *et al.*, 2020). These parameters were extracted from the AUTODYN (Table 3).

2.2. Weldability window calculations

The base of weldability window / criteria needs the collision angle (β) and the collision velocity (V_c). The weldability window is described by Six boarders (Fig. 3). The minimum collision velocity of the weldability window can be calculated by Eq. (4) (Song *et al.*, 2011).

$$R_e = \frac{(\rho_f+\rho_p)V^2_c}{2(H_f+H_p)} \quad (4)$$

where, R_e is equal 10.616, P_f and Pp are the densities of Al1050 in Kg/m^2 H_f and H_p are their Vickers hardness of Al1050.

Table 2. Johnson-Cook parameters of Al 1050 and Steel Ck75 and their Mechanical properties (Khanzadeh *et al.*, 2017; Roudbari *et al.*, 2020)

Materials	Al1050	SteelCk75
A	110	103
C	223	214
M	197	120
Density /kg m^{-3}	2710	7850
Hardness / Hv	30	200
Poisson's ratio	0.33	0.33
Young's modulus / GPa	69	228
Bulk modulus / Gpa	67.4	159
Melting	923.15	1289

Table 3. Jones-Wilkins-Lee Parameters of Anfo (Zerui *et al.*, 2020)

Explosive	Anfo
Detonation velocity/ m s^{-1}	4160
Density /kg m^{-3}	931
E/ G J m^{-3}	2.48
/ Gpa	49.46
/ Gpa	1.891
	3.90
	1.11
ω	0.33

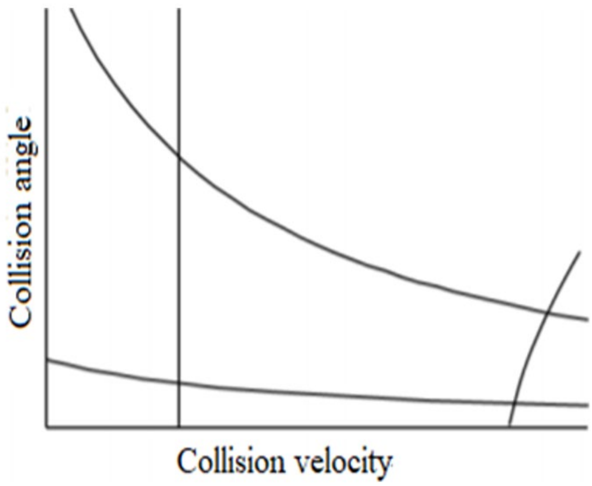

Figure 3. Typical weldability window for EXW (Ribeiro *et al.*, 2014).

The maximum collision velocity (Vc) for the weldability window is 1.2 times the sound velocity

(Yingbin *et al.*, 2017). The minimum collision angle (β) is 2° and the maximum collision angle (β) is 31° (Zakharenko and Zlobin, 1983). The upper border is determined by Eq. (5) (Zamani and Lighat, 2012; Narayan *et al.*, 2019).

$$\mathrm{Sin}\left(\frac{\beta}{2}\right) = \frac{k_3}{(t^{0.25}.V_c^{1.25})} \quad (5)$$

In which β is in radians, t is the thickness of Al1050 in m. The coefficient k3 can be calculated as:

$$k_3 = \left[\frac{E}{12\rho(1\text{-}2\upsilon)}\right]^{½} \quad (6)$$

where ע is Poisson's ratio, E is the elastic modulus expressed in N/mm^2 and ρ is the density in kg/m^2.

The lower border is calculated by Yingbin *et al.* (2017):

$$\beta_{min} = k\left[\frac{H_v}{\rho V_c^2}\right]^{0.5} \quad (7)$$

k is 0.6 for high-quality, H_v is the hardness of Vickers of Al1050, ρ is the density for Al1050 in kg/m^2. Figure 4 is shown the applications of Eqs. (4)-(7) to the collision vs. velocity collision angle space.

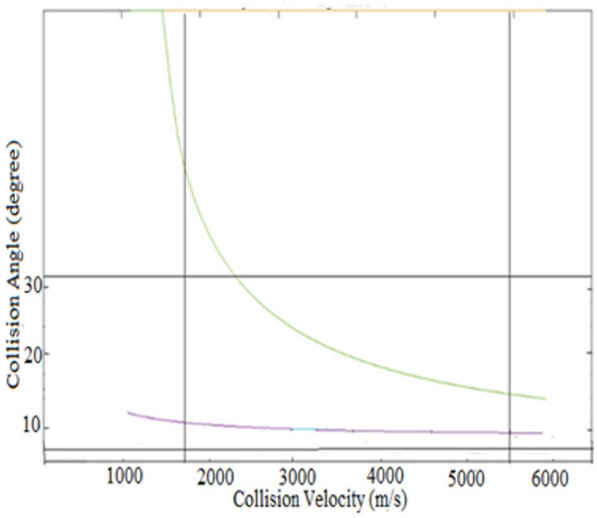

Figure 4. The weldability window for the Al 1050 and Al 1050 (Roudbari *et al.*, 2020).

2.3. Experimental procedure

In this paper, the Al1050 is the flyer plate, and the base plate and Steel Ck75 wire is reinforcement. The Al 1050 plates were bonded by explosive welding process. The bonding was performed using a Steel Ck75 wire among Al 1050. The plates and wires were explosively welded using parallel system for the investigation (Fig. 5).

The measured tensile strength of the Al 1050 plate used was 121 Mpa and Steel Ck75 was 1302 Mpa. The anvil was sand. Anfo was placed in a cardboard box. The detonation was performed by a remote-control system.

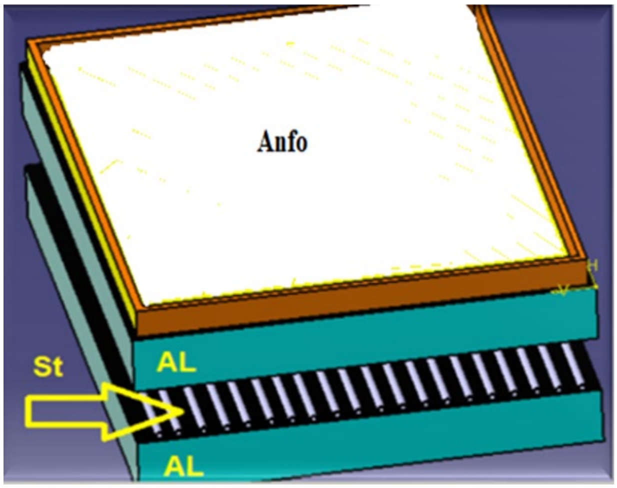

Figure 5. Model of the composite set.

The parameters of the EXW were earned from previews two steps (simulation and weldability window). All the EXW tests performed were simulated.

After the EXW, the samples for metallographic observation were cut perpendicular to the detonation direction. The samples have been paid up to 3000 sandpaper and then polished using 3 microns after that samples of the composite set at room temperature for 30 seconds of etching solution according to the following Table 4 we have.

Table 4. Etching solution for the composite set

Chemical substance	Hf	HNO_3	H_2O
An Amount in millimeters	1.5	3	10

Two tensile specimens were made to define the mechanical properties of the bonding. The tensile test was carried out according to the ASTM E8/E8M (2008) by INSTRON8502 in the tensile state.

3. RESULTS

3.1. Numerical simulation results

The flyer plate and parent plate are paralleled before the explosion. After the explosion, the flyer plate was bent and impacted obliquely with the parent plate (Wang *et al.,* 2011). Figure 6 is shown steps in the simulation of explosive welding.

At first, the flyer plate was accelerated by a shock wave, resulting from explosion pressure, and then by the spread gaseous products of the explosion. If the stand-off distance was sufficiently large, the

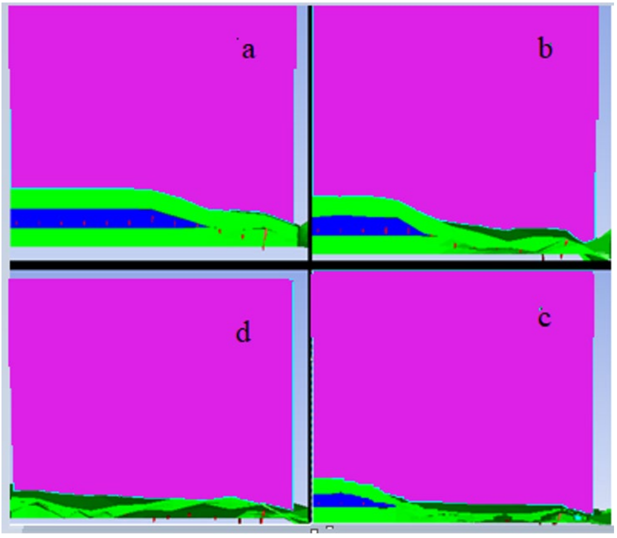

Figure 6. Steps in the simulation of the EXW.

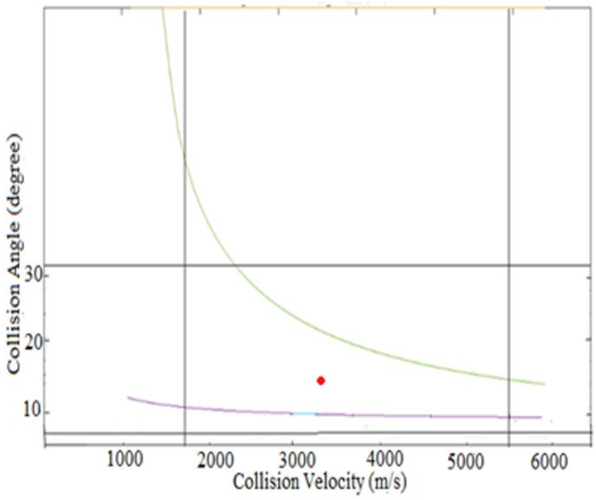

Figure 7. The weldability window of Al 1050/Al 1050 with results of the simulation.

flyer plate finally achieved a final velocity (Akbari Mousavi and Al-Hassani, 2008).

The collide angle is one of the important parameters of the EXW. The collide angle predicted in the simulations. The collision velocity (Vc) in the Autodyne was gotten by dividing the length of the Al by the total timing of the EXW's simulation. In this study, the angle velocity (β) and the collision velocity (Vc) were predicted, respectively, at 3479 $m \cdot s^{-1}$ and 12.1° by AUTODYN.

Numerical simulations were performed to define the appropriate amount of Anfo used in aluminum base composite and the stand-off distance. The stand-off was selected to be about 4 mm. An explosive Rate of R= 6 was found at a suitable rate. Explosive Thickness was 60 mm.

3.2. Weldability window results

In this paper, all of the parameters are plotted in the weldability window, This diagram is drawn based on the simulation results. It can be plotted in both the collision angle and the collision velocity.

The collision velocity and the collision angle of the simulation are placed in the weldability window (Fig. 7). The purpose of drawing the weldability window was to predict the welding state before the explosion

3.3. Metallographic examination

The term explosive welding has been used to explain the process whereby bonding of wire happens. Explosive bonding happens when two plates collide at an adequate speed to reason doughy flow at the interlayer of connection (Bhalla and Willams, 1977).

The Al 1050/Steel Ck75/Al 1050 the EXW was fabricated as shown in Fig. 8. The reinforcing wires are visible in the form of dark circular spots in Fig. 8.

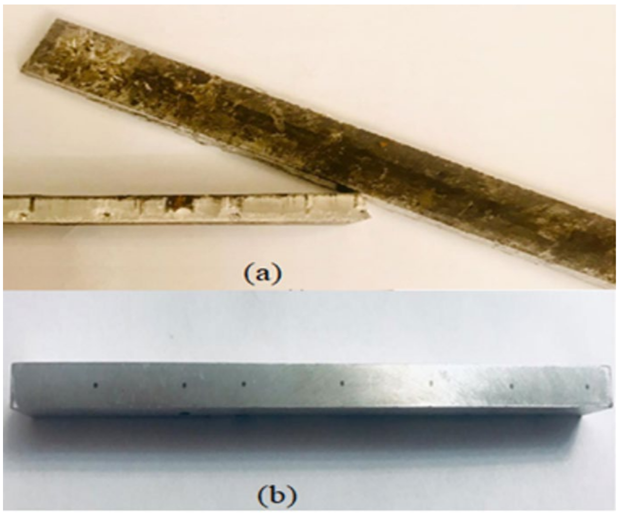

Figure 8. Al/Steel Ck75/Al plate after the explosive welding process: a) after cutting and b) after machining.

The interface bonding Al 1050/Steel Ck75/Al 1050 was tested by the optical microscope. Figure 9 shows the optical microscope images of the bonding interface in different parts. The bonding interface displays that no void bonding faults are observed. The image belongs at the Steel Ck75 wire reinforced Aluminum base composite plate.

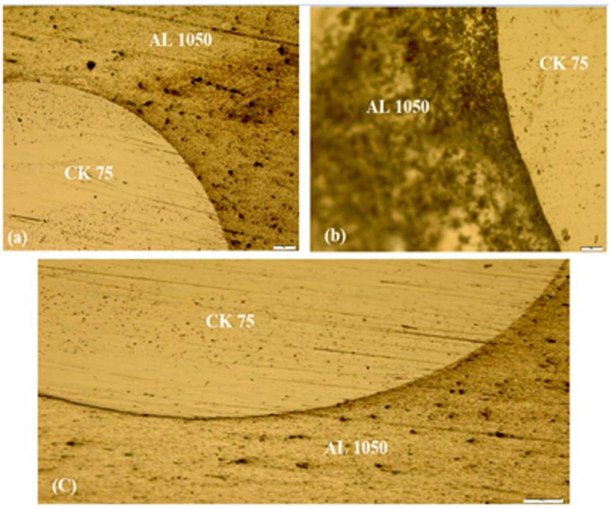

Figure 9. Light microscope image of the bonding at 50 magnifications and different parts.

3.4. Tensile test results

Figure 10 shows the images of test specimens after the tensile test. Strain – Stress curves for unreinforced Al 1050 plates and Steel Ck75 wire reinforced Al1050 plates are shown in Fig. 11 and Fig. 12, respectively. The results of the tensile testing are shown in Table 5 and in Fig. 13.

The Al/Steel/Al shows the rather improvement in the yield strength and ultimate tensile strength as compared to Al/Al composites. This is possibly due to good interface bonding among Steel and Aluminum. The good interface helps in load transfer from Aluminum to Steel during tensile testing (Pakzaman and Divandari, 2012). Aluminum base composite without reinforced result in the lower improvement in strength.

Figure 10. Fracture of the specimens after the tensile test.

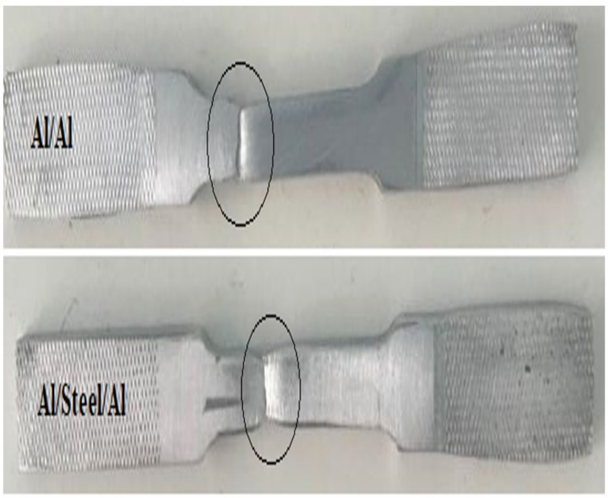

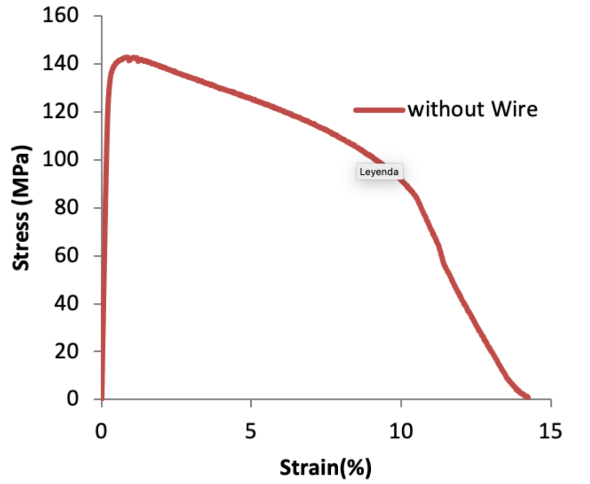

Figure 11. Stress/Strain curve for Al/Al.

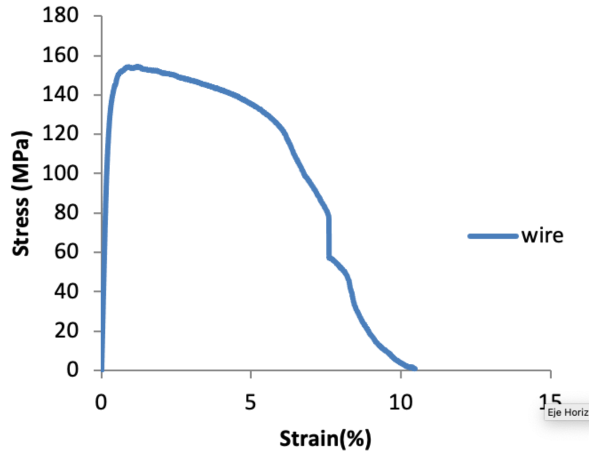

Figure 12. Stress/Strain curve for Steel Ck75 wire reinforced Al/Al.

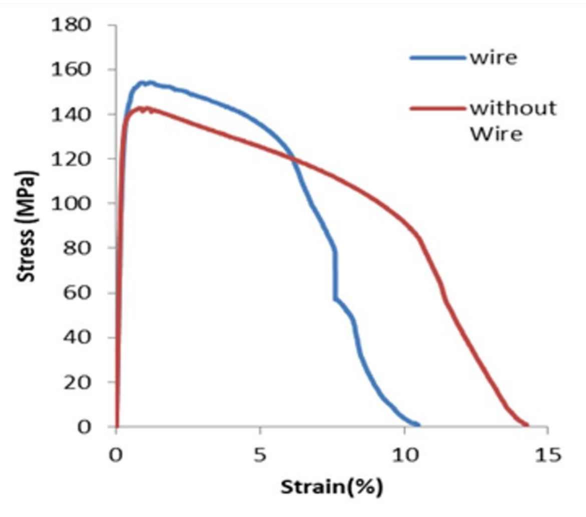

Figure 13. Relation of tensile specimens of Al/Al and Al/Al reinforced with wire.

Table 5. Properties of the composite specimens for the tensile test

Materials	Yield strength (MPa)	Ultimate tensile strength (MPa)
Al/Al	139	142.5
Al/Steel Ck75/Al	143	154.5

4. DISCUSSION

Interconnected Steel Ck75 wire reinforced Aluminum base composite was successfully prepared by the explosive welding process. Thus, it seems that the weldability window and the simulation are useful for earing all parameters of explosive welding. The simulation permits voluntary exchange in the parameters without extra cost.

The communication between the numerical simulation and the experiment shows that all parameters are suitable, the stand-off is 4 mm, an explosive Rate of R=6 and the thickness of the explosive is 60 mm.

The aim of the weldability window to predict the welding state before the detonation. Then, using the simulation software, the angle of collision and the impact of velocity were achieved. Subsequently, the help of the weldability window and simulation were determined the exact position of the weld before the explosion and the number of tests reduced.

Thus, it shows that the sample is good to simulate the EXW. The parameters are reasonable to earn from the numerical study.

In this paper which was performed to increase tensile strength, thus, the highest strength was gotten for the reinforced wire composite. Al 1050/Al 1050 sample while the lowest strength was gotten for unreinforced Al 1050/Al 1050 sample. It was observed that the Steel Ck75 wire reinforced composites show maximum improvement in strength among the composite.

The quality of the interface steel wire could improve strength from 142.5 to 154.5 Mpa, and yield strength was increased from 139 to 143 Mpa. Roudbari *et al.* (2020) manufactured Steel 1006 wire reinforced Aluminum base composite through explosive welding, and their connection displayed no fracture or no melting layer.

5. CONCLUSIONS

- In this study, the weldability window of Al 1050/Al 1050 was plotted. On this basis, Aluminum base composite is reinforced with Steel Ck75 wires by explosive welding. The bonded Al/Steel Ck75/Al by explosive welding was successfully and the bonding didn't also show any crack or fault.
- In conclusion, the weldability criteria and the simulation were successfully considered to predict the suitable welding parameters to catch excellent bonding.
- The improvement in tensile properties is strongly dependent on the wire reinforced composites. Tensile tests have shown that the steel wire reinforced Aluminum base composites have satisfactory mechanical properties in that the ultimate tensile strength increases by 8.5% compared to Al/Al.

REFERENCES

Akbari Mousavi, S.A.A., Al-Hassani, S.T.S. (2008). Finite element simulation of explosively-driven plate impact with application to explosive welding. *Mater. Design* 29 (1), 1–19. https://doi.org/10.1016/j.matdes.2006.12.012.

ASTM E8/E8M (2008). Standard test methods for tension testing of metallic materials. ASTM International, West Conshohocken, PA, USA.

Bhalla, A.K., Willams, J.D. (1977). Production of stainless-steel wire-reinforced aluminum composite sheet by explosive compaction. *J. Mater. Sci.* 12, 522–530. https://doi.org/10.1007/BF00540277.

Deemyad, T., Moeller, R., Sebastian, A. (2020). Chassis Design and Analysis of an Autonomous Ground Vehicle (AVG) using Genetic Algorithm. *Intermountain Engineering, Technology and Computing (IETC)*, 20154025. https://doi.org/10.1109/IETC47856.2020.9249180.

Etemadi, E., Naseri, A., Valinezhad, M. (2020). Novel U-bending designed setups for investigating the spring-back/spring-go of two-layer aluminum/copper sheets through experimental tests and finite element simulations. Proceedings of the Institution of Mechanical Engineers, Part L, *Design and Applications* 234 (8), 1142-1153. https://doi.org/10.1177/1464420720930251.

Gülenc, B., Kaya, Y., Durgutlu, A., Gülenc, I.T., Yildirim, M.S., Kahraman, N. (2016). Production of wire reinforced composite materials through explosive welding. *Arch. Civ. Mech. Eng.* 16 (1), 1-8. https://doi.org/10.1016/j.acme.2015.09.006.

Guler, K.A., Kisasoz, A., Karaaslan, A. (2014). Investigation of Lost Foam Casted Aluminum Bimetal Microstructures. *Mater. Test.* 56 (9), 737-740. https://doi.org/10.3139/120.110625.

Huagui, H., Jichao, W., Wenwen, L. (2017). Mechanical properties and reinforced mechanism of the stainless-steel wire mesh–reinforced Al-matrix composite plate fabricated by twin-roll casting. *Adv. Mech. Eng.* 9 (6), 1-9. https://doi.org/10.1177/1687814017716639.

Khanzadeh, M.R., Bakhtiari, H., Seyedi, M., Ahmadi, H.R. (2017). Simulation and welding window of three layers explosively bonded AA5083 and AA1050 aluminum alloys to carbon steel. *J. Energ. Mater*. 12 (3), 139-152.

Khanzadeh Gharah, S.M., Khalaj, G., Pouraliakbar, H., Jandaghi, M.R., Dehnavi, A., Bakhtiari, H. (2018). Multilayer Cu/Al/Cu explosive welded joints: Characterizing heat treatment effect on the interface microstructure and mechanical properties. *J. Manuf. Process*. 35, 657-663. https://doi.org/10.1016/j.jmapro.2018.09.014.

Los, I.S., Khorin, A.V., Troshkina, E.G., Guskov, M.S. (2010). *Al–Cu composite by explosive welding*. X international symposium on explosive production of new materials: Science, Technology, Business and Innovations (EPNM-2010). Bechichi, Montenegro, pp.1–14.

Mavhungu, S.T., Akinlab, E.T., Onitiri, M.A., Varachia, F.M. (2017). Aluminum Matrix Composites for Industrial Use: Advances and Trends. *Procedia Manuf.* 7, 178-182. https://doi.org/10.1016/j.promfg.2016.12.045.

Narayan, S., Mori. A., Nishi, M., Hokamoto, K. (2019). Underwater shock wave weldability window for Sn-Cu pla-

tes. *J. Mater. Process. Tech.* 267, 152-158. https://doi.org/10.1016/j.jmatprotec.2018.11.044.
Nassiri, A., Chini, G., Vivek, A., Daehn, G., Kinsey, B. (2015). Arbitrary Lagrangian-Eulerian finite element simulation and experimental investigation of wavy interfacial morphology during high velocity impact welding. *Mater. Design* 88, 345-358. https://doi.org/10.1016/j.matdes.2015.09.005.
Pakzaman, H.R., Divandari, M. (2012). Effect of nickel coating on steel wire reinforcement on mechanical properties of aluminum matrix composites produced via lost foam casting. *Proceeding of Iran International Aluminum Conference (IIAC2012).* https://www.civilica.com/Paper-IIAC02-IIAC02_042.html.
Patterson, R. (1993). *Fundamentals of explosion welding*. ASM Handbook, pp. 60-164.
Ribeiro, J.B., Mendes, R., Loureiro, A. (2014). Review of the weldability window concept and equation for explosive welding. *J. Phys. Conf. Ser*. 500 (5), 052038. https://doi.org/10.1088/1742-6596/500/5/052038.
Roudbari, M., Mehdipoor, A., Azarafza, R. (2013). Heat treatment of stainless steel 316L- titanium bimetal manufactured by explosive welding. *IRJABS.* 7 (10), 687-692. http://www.irjabs.com/files_site/paperlist/r_2003_140406222643.pdf.
Roudbari, M., Refahati, N., Mehdipour, A. (2020). Production of steel 1006 wire reinforced aluminum base composite by explosive welding. *Rev. Metal*. 56 (2), e165. https://doi.org/10.3989/revmetalm.165.
Sharma, A.K., Bhandari, R., Aherwar, A., Rimašauskienė, R., Pinca-Bretotean, C. (2010). A. Study of advancement in application opportunities of aluminum metal matrix composites. *Mater. Today Proc.* 26 (Part. 2), 2419-2424. https://doi.org/10.1016/j.matpr.2020.02.516.
Song, J., Raabe, D., Eggeler, G. (2011). Microstructure and properties of interfaces formed by explosion cladding of titanium to low carbon steel. Ph.D. Thesis, Ruhr-University Bochum, Germany.
Wagner, M.X. (2018). Light-Weight Aluminum-Based Alloys—From Fundamental Science to Engineering Applications. *Metals* 8 (4), 260. https://doi.org/10.3390/met8040260.
Wang, Y., Beom, H. G., Sun, M., Liu, S. (2011). Numerical simulation of explosive welding using the material point method. *Int. J. Impact Eng.* 38 (1), 51-60. https://doi.org/10.1016/j.ijimpeng.2010.08.003.
Yingbin, Liu., Chao, Li., Xiaoyan, Hu., Chufan, Y., Tiansheng, L. (2017). Explosive welding of copper to high nitrogen austenitic stainless steel. *Metals* 9 (3), 339. https://doi.org/10.3390/met9030339.
Zakharenko, I., Zlobin, B. (1983). Effect of the hardness of welded materials on the position of the lower limit of explosive welding combust. *Combust. Explos. Shock Waves* 19, 689-692. https://doi.org/10.1007/BF00750461.
Zamani, E., Lighat, G.H. (2012). Explosive welding of Stainless Steel-Carbon steel coaxial pipes. *J. Mater. Sci*. 47, 685-695. https://doi.org/10.1007/s10853-011-5841-9.
Zarabimanesh, Y., Saffari, P.R., Saffari, P.R., Refahati, N. (2021) Hygro-thermo-mechanical vibration of two vertically aligned single-walled boron nitride nanotubes conveying fluid. *Journal of Vibration and Control*. https://doi.org/10.1177/10775463211006512.
Zerui, S., Shi, Ch., Xu, F., Feng, K., Zhou, Ch., Wu, X. (2020). Detonation process analysis and interface morphology distribution of double vertical explosive welding by SPH 2D/3D numerical simulation and experiment. *Mater. Design* 191, 108630. https://doi.org/10.1016/j.matdes.2020.108630.